

1 **A Novel Art of Electrocardiogram Assessment in Zebrafish for Cardiovascular Disease**
2 **Studies and Drug Screening**

3 Tai Le¹, Jimmy Zhang², Anh Hung Nguyen^{1,6}, Ramses Seferino Trigo Torres², Khuong Vo³, Nikil
4 Dutt³, Juhyun Lee⁴, Yonghe Ding⁵, Xiaolei Xu⁵, Michael P.H. Lau⁶, Hung Cao^{1,2,6}

5

6 **Abstract**

7 The zebrafish (*Danio rerio*) has proven to be an excellent animal model for biological research
8 owing to its small size, low cost for maintenance, short generation time, amenable genetics, and
9 optical transparency. Zebrafish have been extensively used in cardiovascular studies in which
10 mutant lines with cardiovascular defects were introduced and analyzed. Despite the small size,
11 technological advances have paved the way to effectively assess cardiac functions of zebrafish.
12 Here, we present a novel art for long-term simultaneous monitoring and analysis of
13 electrocardiogram (ECG) in multiple zebrafish with controlled environment. The system helps
14 minimize the effect of anesthetic drug and temperature to cardiac rhythm side effects as well as
15 save time and efforts by 40-50 fold compared with the conventional approach. We further
16 employed the system to study the Na⁺ sensitivity in the development of sinus arrest in *Tg(SCN5A-*
17 *D1275N)* fish, a study model of the sick sinus syndrome, as well as the relationship between this
18 variant and drug administration. The novel ECG system developed in this study holds promise to
19 greatly accelerate other cardiovascular studies and drug screening using zebrafish.

20

21 **Affiliation**

22 ¹Department of Electrical Engineering and Computer Science, UC Irvine, Irvine, CA, 92697,
23 USA.

24 ²Department of Biomedical Engineering, UC Irvine, Irvine, CA, 92697, USA.

25 ³Donald Bren School of Information and Computer Sciences, UC Irvine, CA 92697, USA.

26 ⁴Department of Bioengineering, University of Texas, Arlington, TX, 76019, USA.

27 ⁵Department of Biochemistry and Molecular Biology, Mayo Clinic, Rochester, Minnesota, 55905,
28 USA.

29 ⁶Sensoriis., Inc, Edmonds, WA, 98026, USA.

30

31

32 **Correspondence**

33 Hung Cao, Ph.D.

34 Assistant Professor of Electrical and Biomedical Engineering

35 University of California, Irvine

36 Irvine, CA 92697

37 E-mail: hungcao@uci.edu

38 Introduction

39 Cardiovascular diseases (CVDs) are the leading cause of death worldwide. According to the 2020
40 AHA Annual Report, almost 860,000 people died of CVDs in the U.S. in 2017, and the overall
41 financial burden from CVDs totaled \$351.2 billion in 2014-2015, emphasizing the urgency to
42 explicate the etiologies of CVDs [1]. One such CVD is the sick sinus syndrome (SSS), a collection
43 of progressive disorders marked by the heart's inability to maintain a consistent rhythm of heart
44 muscle contraction and relaxation [2]. It is characterized by age-associated dysfunction of the
45 sinoatrial node (SAN), with varying symptoms such as syncope, heart palpitations, and insomnia
46 [3]. The SSS has multiple manifestations on electrocardiogram (ECG) recordings, including sinus
47 bradycardia, sinus arrest, and sinoatrial block. The pathophysiology of SSS is not fully
48 understood, but research has determined that it can be caused by numerous factors ranging from
49 pharmacological medications and sleep disturbances to fibrosis and ion channel dysfunction [4].
50 The current primary treatment for SSS is the implantation of an artificial pacemaker. While
51 pacemakers [5] have been effective in treating various arrhythmic conditions [6], they also carry
52 their own complications. Since the pacemaker is seen as a permanent solution, long-term issues
53 such as lead displacement, hematomas, and pneumothorax are significant [7], and conditions
54 such as thromboembolism and stroke are documented [8, 9]. Additionally, because of the
55 multifactorial nature of SSS, new arrhythmic symptoms could arise after pacemaker implantation,
56 as seen in pacemaker syndrome [10]. All these issues could worsen a patient's condition after
57 pacemaker implantation. As a result, permanent alternative solutions should be investigated,
58 including utilizing a biological means to naturally regenerate or replicate the function of the SAN.
59 Previous research has emphasized SSS-associated genetic pathways as potential avenues to a
60 more permanent treatment for SSS. Gene therapy techniques have been utilized to rescue SAN
61 function. Overexpression of *Tbx18* and *Tbx3* via cardiomyocyte transfection has been shown to
62 develop cells with SAN-like function, forming a biologically produced pacemaker. These genes
63 were linked to the expression of connexin proteins, such as *Cx40*, and *Cx43*, which were crucial
64 in maintaining the proper propagation of cardiac conduction [11-13]. Several animal models (*e.g.*
65 mice, rats, pigs) have been tested with this strategy, which have resulted in generally positive
66 results [14-17]. However, gene therapy does have some limitations such as its temporary nature
67 and heterogeneity (not all cells are transfected). Additionally, no study has demonstrated its
68 efficacy in humans, as all studies were conducted in animal models. Therefore, more research
69 should be conducted to identify the electrophysiological phenotypes of these genetic anomalies
70 to help devise future treatment methods.

71 Zebrafish serve as an ideal model for cardiovascular studies because of their similar homology to
72 humans in both morphology, physiology, and genetics. Despite having only two discernible
73 chambers in the zebrafish heart compared to four in human hearts, the zebrafish heart possesses
74 a similar contractile structure with an analogous conduction system [18, 19]. The zebrafish
75 genome also carries remarkable homology to that in humans, as 70% of all human genes have
76 orthologues in the zebrafish genome, making the zebrafish model an applicable model in studying
77 genetic pathways [20]. Therefore, the zebrafish model is appropriate in the study of SSS and the
78 correlation of related genetic pathways to the electrophysical phenotype via ECG. Currently,
79 several research groups have developed zebrafish ECG acquisition and sensors to support
80 cardiac studies. Regarding sensor design, needle electrodes are the most commonly used. Lin *et*
81 *al.*, [21] designed and tested the needle electrode with different materials, including tungsten
82 filament, stainless steel and silver wire to investigate the recorded signal quality. Along with a
83 portable ECG kit, the authors aim to provide a standard platform for research and teaching
84 laboratories. The needle system is also deployed in other studies [21-24] to conduct biological
85 and/or drug-induced research. All needle-based studies demonstrated promising results;
86 however, to collect favorable signals, the needles need to be gently inserted through the dermis

87 of zebrafish. This could cause injury to the fish's heart, thus possibly changing signal morphology
88 [23]. Moreover, it requires an intensive effort in precisely positioning the electrode on the heart to
89 achieve a clear ECG signal. Therefore, several alternative probe systems have been developed,
90 including the micro-electrode array (MEA) and the 3D-printed sensors. Our team and others have
91 demonstrated the use of MEA for acquisition and provided the signal with favorable signal-to-
92 noise ratio (SNR) with high spatial and temporal resolution [25-27]. For instance, we presented a
93 MEA array covering the fish's heart which enables site-specific signals [26, 27]. Cho *et al.*, [28]
94 developed a MEA printed on a flexible printed circuit board (FPCB) based on a polyimide film for
95 multiple electroencephalogram (EEG) recording for epilepsy studies. Although the MEA allows
96 multiple signal recordings, only one fish can be assessed at a time due to the limiting number of
97 channels on acquisition. Moreover, most studies have used bulky and expensive acquisition tools
98 to collect data and then transfer them through a cable to a computer. These require a designated
99 benchtop area to conduct experiments, yet potentially encounters errors due to instability of cable
100 and connectivity. In the market, commercially available systems, e.g. the one from iWORX (Dover,
101 NH) with a compact amplifier, can improve the mobility of the system. However, several
102 challenges have not been resolved: **i)** the current systems only record for a short period of time,
103 which result in inconsistent results among different fish; **ii)** the ECG acquisition requires
104 anesthetized animals, rendering it stressful to the fish and inadequate to provide intrinsic cardiac
105 electrophysiological signals; **iii)** manual one-by-one measurement limits the ability of doing
106 studies required to test with a large number of fish; and **iv)** signal processing has been carried
107 out offline with humongous efforts.

108 In this work, we introduce a novel system, Zebra II, capable of obtaining long-term ECG
109 recordings for multiple fish simultaneously. An in-house electronic device is developed, leveraging
110 the Internet of Thing (IoT) capability with wireless data transmission and data processing on a
111 mobile application. This enhances the mobility and versatility of the system to conduct research
112 on zebrafish models. The system is validated through numerous experiments, showing its
113 potential with 1) simultaneous measurement for up to 4 fish; 2) continuous ECG recording for up
114 to 1 hour compared to several minutes of other systems; 3) reduction in arrhythmic side effects
115 with the use of 50% lower Tricaine concentration. Furthermore, we investigate a specific
116 electrophysiological phenotype, namely sinus arrest, induced by sodium chloride on mutant fish
117 *Tg(SCN5A-D1275N)* to demonstrate that our proposed system can be used as a screening tool
118 to detect and elucidate zebrafish cardiac arrhythmic symptoms.

119

120 Results

121 Demonstration of Zebra II for multiple zebrafish ECG recording

122 The Zebra II system is designed to allow the fish to stay comfortably for up to 1 hour while the
123 ECG signal is acquired. It comprises of a perfusion system, soft polymer housings, sensors and
124 an electronic system (**Fig. 1a**). The perfusion system continuously provides the low concentration
125 of anesthetic drug (MS-222), reducing the aggressiveness and activity of zebrafish and giving the
126 fish with adequate oxygen levels. Thus, with apparatuses made of polydimethylsiloxane (PDMS),
127 the perfusion system can keep them stable for a long time during the measurement. Moreover, a
128 home-made thermo box is designed with a thermostat control, a light bulb, and a temperature
129 sensor, which automatically controls the temperature of environment to conduct experiments. An
130 in-house electronic system and a mobile application are fully developed, allowing wireless data
131 transmission as well as data storage and analysis, thereby greatly reducing time and effort. (**Fig.**
132 **1b-d, Sup. Fig. 1**). The overall fish ECG system specification is shown in **Sup. Table 1**. Finally,
133 the data are wirelessly transmitted to a mobile application as shown in **Fig. 1d**. The mobile app
134 allows real-time data transmission and send the data to the cloud system. The data transmission
135 is further illustrated in **Sup. Fig. 2**.

136 Numerous experiments were conducted to validate the performance of Zebra II. First, the
137 zebrafish ECG was collected simultaneously by the Zebra II and a commercial device developed
138 by iWORX (Dover, NH). The signals were then compared in both frequency domain and time
139 domain (**Sup. Fig. 3a&b**). Specifically, the correlation coefficients were 98.78% and 96.54% in
140 time domain and frequency domain, respectively. Moreover, the heart rate value and QRS interval
141 were also compared (**Sup. Fig. 3c&d**). As seen, the Zebra II's performance is comparable to that
142 of the commercial iWORX device. Further, we performed another experiment on 36 wildtype (WT)
143 zebrafish dividing to 2 groups: 1) control (n = 20) and 2) Amiodarone treated (n = 16) fish.
144 Amiodarone is used to prevent various types of arrhythmic symptoms, including ventricular
145 tachycardia and atrial fibrillation [29]. However, Amiodarone has been also reported to cause
146 bradycardia and to prolong the QT interval in zebrafish [30]. This experiment allowed us to assess
147 the drug screening capacity of the Zebra II system. Specifically, for the treated group, fish were
148 treated with 100 μ M Amiodarone by immersing them in a tank with 200 mL of the Amiodarone
149 medium. ECG was recorded after 1 hour of immersion. This experiment was conducted with both
150 our Zebra II and iWORX systems. As shown in **Sup. Fig. 4**, heart rate (HR) value, QRS duration
151 and QTc interval were analyzed. With the control group, there is no significant difference (p-value
152 > 0.05) between two systems in terms of QRS and QTc value. Similarly, the HR value and QTc
153 value show no significant difference in treated group. Furthermore, the Bland Altman analysis in
154 **Sup. Fig. 4b, d, f** shows the agreement level between two systems with most of HR values and
155 QTc values belonged to the limit of agreement (LOA) region.

156 Investigation of tricaine and temperature to reduce cardiac rhythm side effect

157 As shown in **Fig. 2a**, the ECG morphology was observed with different doses. The ECG signal
158 shows gill motion noise, interfering ECG waveforms such as P, T and QRS waves with 75 ppm
159 Tricaine while the signal appears to be more stable under 100 ppm and 150 ppm treatment,
160 providing clear ECG waves. After 40-min long measurement, the recovered time and survival rate
161 of fish are collected (**Fig. 2b**). It was found that fish under higher Tricaine concentration need
162 longer recovery time. Specifically, it takes the average of 7 minutes to recover the fish under 150
163 ppm while those under 75 ppm and 100 ppm treatment it requires 3 minutes and around 4.2
164 minutes for fish to wake up after measurement, respectively. Furthermore, with 150 ppm
165 treatment, the survival rate is about 75% while other concentrations can keep the fish alive after
166 measurement above 90%. It reflects to the effect of a high dose used under a long period of time
167 measurement which is similar to the dose for fish euthanasia (*i.e.*, 168 ppm) [31]. Given the

168 recovery time and survival rate along with ECG morphology collected for different Tricaine
169 concentrations, the dose of 100 ppm is the optimal one for the prolonged measurement.
170 Regarding the heart rate variation every 5 minutes during the measurement, we characterized it
171 with the ECG signal under 75 ppm and 100 ppm (**Sup. Fig. 5**). After 100 ppm treatment, the heart
172 rate variation shows no significant difference among first 30 minutes, making the average
173 standard deviation (STD) of 17 beats per minute (BPM). In contrast, that value with the ECG data
174 under 75 ppm describes the changes among every 5-minute data, which leads to 22 BPM
175 difference based on STD.

176 Given the optimal Tricaine concentration, different temperatures are investigated. A temperature-
177 control incubator was designed for the experiment. The zebrafish ECG system was put in the
178 middle of the incubator. Temperature within the chamber could range from 20°C to 32°C, as
179 measured by a thermometer inside the chamber and controlled by a thermostat with accuracy of
180 $\pm 1^\circ\text{C}$. Prior to recording the ECG signals in this experiment, the impedance of the electrodes was
181 measured on zebrafish skin (**Sup. Fig. 6**) ensuring the signal stability during the long-term
182 measurement. As shown in **Fig. 2c**, the SDANN at 26°C has the lowest value with the range of
183 36 msec to 75 msec while that at 24°C is highest with the range of 50 msec to 139 msec.
184 Moreover, the data distribution from heart rate value collected by every 5 minutes collected at
185 26°C is the most condensed (**Fig. 2d**). Thus, under 26°C, the heart rate is more stable than that
186 under other temperatures.

187 **Response analysis to drug treatment in real time with the Zebra II system**

188 As shown in **Fig. 3a**, 4 fish were measured simultaneously, and 4 doses were consecutively filled
189 in the reservoir and each dose lasted around 5 minutes. The change in response to different
190 dosages in all four fish was obvious. Zooming out the data collected from fish 1 in different
191 amiodarone dosages as denoted from (1) to (4), the QTc interval showed considerable changes.
192 For instance, the QTc value is 310 msec without drug treatment and it tends to increase after the
193 fish got treated. Specifically, it is 330 msec with 70 μM of amiodarone while it is 476 msec and
194 536 msec with 100 μM and 200 μM of amiodarone, respectively. **Fig. 3b** describes the overall
195 changes in terms of QT prolongation, QRS interval and HR value in response to different
196 amiodarone concentration. With the increase of amiodarone dosage, QT prolongation and QRS
197 interval shows an increase while the average heart rate is decreased.

198 **Evaluation of Na⁺ sensitivity in the development of sinus arrest (SA) in *Tg(SCN5A-* 199 ***D1275N***)**

200 WT fish (n = 12, aged 1.5 years) and *Tg(SCN5A-D1275N)* fish (n = 8, aged 10 months) were used
201 in this experiment. **Fig. 4a** illustrates the ECG morphology of *Tg(SCN5A-D1275N)* with different
202 NaCl dosages. We noticed that with a small NaCl dosage (0.1 ‰), the zebrafish starts showing
203 the reduction in heart rate, followed by significant decrease in higher dosages. According to the
204 SA criteria (*i.e.*, RR interval is greater than 1.5 sec) determined in our previous work [32], sinus
205 arrest appears more frequently after treatment with 0.6 ‰ NaCl and above (**Table 1**). As shown
206 in **Fig. 4b**, the HR value started significantly dropping in 0.6 ‰ NaCl treatment in the SSS mutant.
207 In contrast, NaCl does not show profound effect to the control group (WT fish) as evidenced by
208 the slight decrease in the HR responding to different NaCl levels. It was worth noting that these
209 WT fish were at 1.5 years old, which could attribute to an increase of SA [32], causing the slight
210 reduction of HR in the experiment (**Sup. Fig. 7**). In terms of heart rate variability (HRV),
211 *Tg(SCN5A-D1275N)* fish showed a remarkable increase with the high NaCl dosages (0.9 and 1.8
212 ‰) compared with other dosages. This provides evidence that the *Tg(SCN5A-D1275N)* triggers
213 more sinus arrest under NaCl treatment (**Table 1**). Moreover, QTc interval was also characterized

214 and it shows the same pattern happened in SDNN with the increase of QTc in response to NaCl
215 dosages (**Fig. 4d, Sup. Fig. 8**).

216 As mentioned previously, the sodium channel gene *SCN5A* is one of the most frequently mutated
217 genes in LQTS. To further investigate this variant as a candidate for cardiac studies, we assess
218 the relationship between *SCN5A* and methamphetamine (Meth) – a controlled substance. Several
219 groups have studied its connection of using addictive drugs with sudden death. For instance,
220 Sayaka, *et al.*, screened several variations in the LQTS-associated genes *KCNQ1* (*LQT1*) and
221 *KCNH2* (*LQT2*) showing the link to the risk of serious cardiac arrhythmia for those abusing
222 addictive drugs [33]. However, the authors do not test for *SCN5A* variants which provided us an
223 opportunity to explore its effect. Additionally, we sought to rescue the bradycardic symptoms
224 induced by NaCl to provide insight on the nature of those symptoms, as Meth has been previously
225 demonstrated to increase heart rate after administration [34]. Specifically, we treated two groups
226 (control – WT fish and treated – *Tg(SCN5A-D1275N)*) in 0.9 ‰ NaCl in 30 minutes before
227 immersing the fish in 50 µM Meth in other 30 minutes. As shown in **Fig. 5**, the HR value, SDNN
228 and QTc value were compared between two groups with three critical moments, including without
229 drug treatment, with NaCl treatment and combined NaCl and Meth treatment ($n = 12$ WT fish and
230 $n = 8$ *Tg(SCN5A-D1275N)*). The average heart rate after the combined NaCl and Meth treatment
231 (96.96 ± 7.61 BPM) showed a slight increase compared with that solely treated with NaCl (94.59
232 ± 5.69 BPM) with *Tg(SCN5A-D1275N)*; however, it showed no significant difference between two
233 moments ($P > 0.05$). Similarly, the SDNN value does not show any significant difference. This
234 means the Meth treatment did not affect the HR and SDNN in both groups (**Table 1**), implying
235 that NaCl administration resulted in irreversible bradycardic symptoms that could not be easily
236 treated with agents that increase heart rate. In contrast, we found a significant increase of QTc
237 interval in the *Tg(SCN5A-D1275N)* group before (360.1 ± 64.0 msec) and after (391.3 ± 76.1
238 msec) Meth treatment, indicating the additive effect of Meth to QT prolongation (**Table 1**- in red).

239

240 Discussion and Conclusion

241 A strong association between high sodium intake and cardiovascular disease has been reported
242 in hypertensive populations [35]. A high sodium diet is associated with alterations in various
243 proteins responsible for transmembrane ions homeostasis and myocardial contractility. Recent
244 studies provided important evidence that excess sodium promotes structural and functional
245 impairment of the heart, especially in populations bearing mutant phenotypes of the major cardiac
246 sodium channels. These mutations are responsible for various types of cardiac disorders,
247 including Brugada syndrome (*BrS*), long QT syndrome (*LQT3*), cardiac conduction disease
248 (CCD), sick sinus syndrome (SSS), atrial fibrillation (AF), progressive cardiac conduction defect
249 (PCCD) [36]. In the original reports [36-39], *SCN5A* mutations are associated with cardiac
250 conduction defect and atrial arrhythmias which cause bradycardia with reduced heart rate. In the
251 present study, the developed system shows the susceptible effects of excess sodium ions to
252 abnormal cardiac rhythm of the *Tg(SCN5A-D1275N)* mutant, to validate our system with different
253 arrhythmic phenotypes. Our noticeable finding is that the excessive sodium ions cause sinus
254 arrest in *Tg(SCN5A-D1275N)* at 0.6 ‰, 0.9 ‰, and 1.8 ‰, corresponding to 1.53 sec, 1.55 sec
255 and 1.52 sec, respectively; and slower heart rate and prolonged QTc are observed only in mutant
256 fish. These results provide a significant association between the increased frequency of sinus
257 arrest, slower heart rate, and prolonged QTc with increased sodium intake in SSS mutants.
258 According to previous reports [40, 41], the *SCN5A* sodium-channel protein can disrupt the heart's
259 electrical activity and lead to a dramatic decrease of heart rate. The slow-conducting *Tg(SCN5A-*
260 *D1275N)* phenotype has been proved by voltage-clamp measurement [42, 43] in which data were
261 consistent with our finding. In the eight fish *D1275N* carriers, the average QTc intervals were 385
262 msec at the upper physiological limit, indicating that the QTc intervals in *Tg(SCN5A-D1275N)* fish
263 are generally more prolonged than wild type animals. Moreover, excess Na⁺ ions cause not only
264 slow heart rate and prolonged QTc but also increased sinus arrest frequency in *Tg(SCN5A-*
265 *D1275N)* (**Fig. 4**).

266 Sodium-overload sinus arrest observed in this study may be associated with a rise of the
267 intracellular Na⁺ in heart muscle due to gain-of-function of *Tg(SCN5A-D1275N)* for sodium ions
268 traveling into the cell. Detection of Na⁺-induced sinus arrest by the developed system shows that
269 Brugada syndrome mutation *Tg(SCN5A-D1275N)* is susceptible to excess Na⁺ ions due to
270 hastening epicardial repolarization and causing idiopathic ventricular conduction, which induce
271 ECG changes and ventricular arrhythmias of Brugada syndrome. Moreover, the mutation
272 (*D1275N*) evokes the long QT syndrome which is caused by excessive I_{Na} detected by the
273 developed system with continuously prolonged measurement. Recorded data by the developed
274 system is consistent with clinical reports indicating that Brugada syndrome in human and animals
275 have reported Na⁺-induced abnormalities in ventricular conduction [44, 45]. Thus, an overload of
276 Na⁺ ions can cause destabilized closed-state inactivation gating of *D1275N* that may attenuate
277 the ventricular conduction delay, shown in arrhythmic parameters (**Table 1**).

278 One of the key novelties of the Zebra II system is the capacity to test multiple drugs on one fish
279 with a continuously prolonged assay. The analysis of ECG of *Tg(SCN5A-D1275N)* indicates that
280 Methamphetamine do not improve sinus arrest frequency and heart rate. However, it caused
281 prolonged QT at 50 μM of Meth. In both groups, the QTc was longer (by 350 msec for wild type
282 and 385 msec for *Tg(SCN5A-D1275N)* after Methamphetamine treatment. Thus, the robust
283 performance of the system allows incorporation the multiple drugs with different effects (e.g.,
284 antagonistic effects) in a single continuously prolonged assay to study drug-drug interactions on
285 a specific arrhythmic phenotype, which is heavily performed by the short time course of current
286 systems. Extending ECG measurement in merely-sedated fish allows measuring interactive
287 effects of different drugs on a specific phenotype by a prolonged screening course. Different ECG
288 phenotypes are recorded using the prolonged real-time courses (over 40 min) to provide intuitive

289 insights into how the drug interaction effects, indicating a tool to evaluate drug efficacy. As shown
290 in **Fig. 4d**, the average SDNN, the standard deviation of normal to normal R-R intervals, was 125
291 msec for wild type fish, but was 255 msec for *Tg(SCN5A-D1275N)*, consistent with reduced
292 conduction velocities due to Na⁺ ion channel disfunction [46].

293 The number of conduction defects associated with the *D1275N* mutation provide a
294 biophysiological mechanism for conduction defects observed in *Tg(SCN5A-D1275N)* and
295 analyzed by the developed system. The *D1275N* mutant channels provides new evidence that
296 excess Na⁺ ions in mutant sodium channel dysfunction can produced isolated conduction disease,
297 with pathological slowing of the heart rate, prolonged QTc and higher frequency of sinus arrest.
298 Although functional data are not available for the system performance, consistent data of
299 conduction disease and Na⁺ channel function in real-time and prolonged continuously
300 measurement indicates that the developed system can be used for many applications including
301 drug screening and interactions with various zebrafish mutant phenotypes.

302 In order to enable remote monitoring and high-throughput zebrafish ECG analysis, our data
303 pipeline is deployed on a cloud server. This further facilitates a collaborative platform for different
304 research groups regardless of their geographical locations. Based on the state-of-the-art in the
305 Internet of Things (IoT) [47, 48], we have designed and implemented a robust and scalable real-
306 time stream processing system leveraging Google Cloud infrastructure. The architecture is
307 illustrated in **Sup. Fig. 9**. The IoT Core provides the functionalities to manage and configure
308 connected devices conveniently and securely. Once the ECG signal is acquired from the
309 measurement device, it is transmitted in real-time to the cloud platform through the Message
310 Queuing Telemetry Transport (MQTT) protocol. The MQTT protocol is designed to maintain a
311 long-lived connection between the device and the client with minimal communications overheads
312 to save bandwidth for data transmission. Cloud Pub/Sub is an asynchronous communication
313 medium between the device and the servers on the IoT cloud. The communication is based on
314 the notion of topics that cache durable messages. Zebrafish ECG published on a certain topic by
315 the device can be pushed to or pulled from the servers that subscribe to the same topic for storage
316 and analytics.

317 The storage layer is responsible for storing the real-time zebrafish ECG into the database. As one
318 of the most promising time-series databases, InfluxDB is employed in our proposed system for
319 timely and reliable storage. As an advanced non-relational database, InfluxDB resolves the
320 performance bottleneck of traditionally used databases such as MySQL, and provides greater
321 flexibility and read-write speed. In the analytics layer, Cloud Functions, a serverless execution
322 environment, run processing techniques such as denoising, filtering, normalizing, detecting P
323 wave, QRS complex, or T wave, and extracting other useful features. Furthermore, machine
324 learning approaches can be applied to these data with the aid of the Kubernetes Engine to train
325 and deploy the models in containerized applications. Computationally intensive process and
326 analysis tasks are carried out in powerful servers, which greatly eases the burden of local devices.

327 The graphical user interface is responsible for data visualization and management. It provides
328 easy access to the data in the IoT cloud. Grafana is an open platform for monitoring time series
329 data that we utilize to design dashboards to represent the ECG signals. Users can log onto the
330 cloud to acquire visualized ECG data on either web pages or mobile applications. Based on the
331 results of data analysis, we can observe and understand the real-time conditions of zebrafishes.
332 In the event of any anomalies or suspicious readings, the IoT cloud will notify users in time.

333 The prolonged continuous ECG performance increases diagnostic and monitoring yield in the
334 detection of asymptomatic cardiac events and reduces ECG artifact that improves arrhythmia
335 detection. Moreover, it improves the quality and quantity of data collected from mutation-related
336 sick sinus syndrome and arrhythmia during cardiac drug screening as well as increase zebrafish

337 compliance provided by prolonged continuous ECG monitoring. However, we have also observed
338 some limitations with our system. After conducting various experiments, we noticed that the
339 electrode placement significantly contributes to the quality of ECG signal. With the use of the low
340 Tricaine concentration to enable longer ECG recording, the fish tended to exhibit unexpected
341 strong movement, thus leading to the electrode dislocation. Moreover, measuring multiple fish
342 simultaneously required a great effort in aligning the electrode on the fish's chest to acquire
343 favorable ECG signal. The dripping setup used to continuously provide low Tricaine solution
344 sometimes caused interferences to the ECG signal due to the inconsistency of its flow rate. To
345 address these, we are planning to measure the real-time impedance of electrode-body interface
346 and use that as the feedback information to control the electrode. We also plan to control the flow
347 rate and provide a dedicated heating system to precisely control the medium temperature.

348 In conclusion, we have successfully demonstrated the novel Zebra II ECG system for multiple
349 adult zebrafish. The major novelties lie in the long period (up to 1 hour) for recording of multiple
350 fish, the minimal side effects, the automated cloud-based analytics as well as all other controlled
351 features. We have demonstrated and further deployed the system for phenotyping cardiac
352 mutants in response to various drugs and environmental cues treated simultaneously.
353 Specifically, we have utilized our system to study Na⁺ sensitivity of the variant *SCN5A-D1275N*,
354 for the first time, by observing changes in the frequency of sinus arrest episodes, heart rate value
355 and QTc value. This is extremely important as it may provide answers for millions of cases of
356 sudden death due to cardiac arrest. The Zebra II can be used for a host of cardiac disease studies
357 and drug screening applications using the zebrafish model.

358

359 **Methods**

360 **Mutant line *Tg(SCN5A-D1275N)* and zebrafish husbandry**

361 Mutant line *Tg(SCN5A-D1275N)*, a transgenic zebrafish arrhythmia model bearing the pathogenic
362 human cardiac sodium channel mutation *SCN5A-D1275N*, was used to characterize and validate
363 device performance, study sinus node dysfunction, and perform drug high throughput screening
364 assays. Correlation between clinical phenotype and the mutant line has been reported for
365 bradycardia, conduction-system abnormalities, episodes of sinus arrest [32].

366 Adult wild/mutant-type zebrafish with the age from 13 to 20 months (body lengths approximately
367 3-3.5 cm) were used in this study. Zebrafish are kept in a circulating system that continuously
368 filters and aerates the system water to maintain the water quality required for a healthy aquatic
369 environment. The fish room located in Engineering Gateway #3324 at UC Irvine is generally
370 maintained between 26-28.5°C and the lighting conditions are controlled with 14:10 hours (*i.e.*,
371 light: dark).

372 All animal protocols in this study were reviewed and approved by the Institutional Animal Care
373 and Use Committee (IACUC) protocol (#AUP-18-115 at University of California, Irvine). All
374 experiments were performed in accordance with relevant guidelines and regulations.

375 **Drug Administration**

376 To anesthetize fish, we used a buffered solution of 200 parts-per-million (ppm) Tricaine (Sigma,
377 USA) [49]. The Tricaine was dissolved in distilled water to a final concentration of 7,000 parts-
378 per-million (ppm) as a stock, and the pH value was adjusted to 7.2 with sodium hydroxide (Sigma).

379 Amiodarone (Sigma) was dissolved in water at 65°C for 2 h and stocked as 900 µM at 4°C. Before
380 use, the solution was re-dissolved at 65°C for 1 h [50]. The fish were immersed in a tank with 100
381 µM amiodarone for 1 hour and then return to fish water in 15 mins before doing experiment.

382 *SCN5A* is the gene associated with the alpha subunit of the voltage-gated sodium channel protein
383 $Na_v1.5$. Primarily responsible for the induction of the cardiac action potential, the $Na_v1.5$ channel
384 has been linked to several arrhythmogenic diseases such as sick sinus syndrome, long QT
385 syndrome (LQTS), and Brugada syndrome [51]. Numerous studies have documented the
386 molecular interactions and pathways involved with $Na_v1.5$ as well as the various disease
387 phenotypes exhibited by $Na_v1.5$ variants [51, 52]. However, there is a current lack of functional
388 characterization in regard to the molecular dynamics of $Na_v1.5$ variants, including the functional
389 response of $Na_v1.5$ to initiate action potentials based on variation of sodium concentration. To the
390 best of our knowledge, there are no research studies established to investigate the Na^+ sensitivity
391 in the development of sinus arrest. Therefore, an experiment was devised to determine the Na^+
392 sensitivity of the variant *SCN5A-D1275N* by observing changes in the frequency of sinus arrest
393 episodes, heart rate value and QTc value in the transgenic fish after treatment of 0.1, 0.3, 0.6,
394 0.9, and 1.8 ‰ of 5 M NaCl.

395 **Design of the Zebra II**

396 The Zebra II comprises of a perfusion system, apparatuses, sensors and an in-house electronic
397 system (**Fig. 1a**). The perfusion system comprises four syringes, four valves and tubing. Four
398 syringes contain low dose Tricaine solution, continuously providing the solution to the fish through
399 the tubing system to reduce the aggressiveness and activity of zebrafish but keep them awake.
400 Four valves adjust the solution's flow rate within a range of 5.5 - 6 ml/min [53]. Housing
401 apparatuses and sensors are improved from the previous work [53]. Specifically, multiple small
402 housings are made of polydimethylsiloxane (PDMS), providing comfort to the fish and thus
403 minimizing unwanted artifacts. Moreover, the top and bottom of the apparatus are designed in
404 such a way that the fish can lay comfortably on electrodes with curved shape in the bottom. The

405 top has a redundant part sticking on the wall to keep the fish from escaping the apparatus. With
406 the thermo box, a specific temperature is set by the thermostat control and the light bulb is turned
407 on so that the box's temperature can be maintained at the setup temperature and vice versa.

408 An in-house electronic system and a mobile application are described in **Fig. 1b-d, Sup. Fig. 1**.
409 Specifically, the system includes a system on chip (SoC) supporting Bluetooth Low Energy (BLE),
410 an analog front-end for zebrafish ECG signal acquisition, and a power-supply module with charge
411 management. The SoC adopted nRF52832 from Nordic (*Trondheim, Norway*), which was a 64-
412 MHz Arm Cortex-M4 CPU with a built-in BLE module. The analog front-end of ADS1299 from TI
413 is well-known for biopotential measurements with eight low-noise, programmable gain amplifiers
414 (PGAs) and eight high 24-bit resolution Delta-Sigma ADCs. Its high bit resolution provides both
415 precision and dynamic range, allowing it to capture signals as high as 4.5 V and as low as 0.5 μ V.
416 The data rate is configurable from 250 samples per second (SPS) to 16 kSPS for all eight
417 channels. Digital signals are sent from the ADS modules to the microcontroller for preprocessing
418 via SPI interface. Data ready pin of ADS1299 module is triggered to signal microcontroller once
419 a new data package is ready to transfer. Since multiple zebrafish are recorded simultaneously,
420 differential mode configuration is utilized in the ADS1299. This would preclude signals in each
421 fish from affecting each other. Moreover, a bias electrode with a signal generated by an ADS1299
422 chip is used, enabling a feedback loop built in the chip to get better common mode rejection.

423 **Investigation of tricaine and temperature to reduce cardiac rhythm side effect**

424 As an important vertebrate model, zebrafish have been studied at both the embryonic and adult
425 stages. Anesthesia is used in every experimental procedure to avoid discomfort, stress or pain.
426 The most commonly used anesthetic drug is Tricaine (MS-222) and zebrafish usually are treated
427 with 200 ppm in 3-5 minutes before experiment. However, this drug has been shown to affect
428 cardiac function of the adult zebrafish and decrease the heart rate of the sedated subjects [21,
429 54]. As a result, MS-222 may skew the measurement of zebrafish physiological parameters.
430 Moreover, temperature has profound effects on the performance and biogeography of ectothermic
431 animals including fishes, partly through its effects on metabolism. At low temperatures (*e.g.*, 18 -
432 20°C), myocyte activity is reduced as a natural adaptive mechanism to aid survival during colder
433 climates or reasons [55], which leads to a reduction in heart rate. At higher temperatures,
434 increased heart rate facilitates greater cardiac output to support a higher metabolic
435 activity/demand for oxygen consistent with normal biological rate function. Therefore, with an
436 optimal environment temperature, the proposed prolonged ECG system will help to lower the
437 tricaine concentration which can reduce the cardiac rhythm side effect as well as maintain the
438 ECG morphology. Three different Tricaine concentrations (*i.e.*, 75, 100, and 150 ppm) were used
439 which account for 37.5%, 50% and 75% of original dose (200 ppm), respectively. Eight fish are
440 used for each concentration group.

441

442 **Response analysis to drug treatment in real time with the Zebra II system**

443 As a prominent vertebrae model for disease, zebrafish has already contributed to successful
444 phenotype-based drug discovery, acting a bridge between in vitro assays and mammalian in vivo
445 studies [56-58]. After establishing the optimized ECG assay conditions (*i.e.*, tricaine
446 concentration, and temperature), the Zebra II demonstrated its potential in response to drug
447 treatment in real time. The amiodarone drug was used in this experiment to demonstrate the drug
448 screening capability of the system as it can affect ionic channels, associated with the potential for
449 QT interval prolongation in the heart's electric cycle. With different dosage (*i.e.*, 70 μ M, 100 μ M
450 and 200 μ M) consecutively treated for zebrafish, we can trigger the phenotype of QT interval
451 prolongation to appear and vary in response to the drug treatment.

452 **Signal processing and statistics**

453 The recorded ECG data were analyzed, and several parameters were extracted, including HR,
454 QT, QTc intervals [49]. The standard deviation of normal sinus beats (SDNN) was used to
455 evaluate the short term recording (5 minutes) beat-to-beat variance of HR and the standard
456 deviation of the average normal-to-normal (NN) intervals for each of the 5 min segments (SDANN)
457 was used for prolonged measurement (40 minutes) [59].

458 Statistical analysis was performed by using OriginLab 2019. Specifically, differences between
459 samples were tested with student's t-test and statistical significance accepted at a threshold of P
460 < 0.05 . Multiple comparisons were tested with one-way ANOVA and significant results ($P < 0.05$)
461 were analyzed with pairwise comparisons using Student's t-test applying significance levels
462 adjusted with the Bonferroni method. Significant P-values are indicated with asterisks (*) with * P
463 < 0.05 , ** $P < 0.01$ and *** $P < 0.001$. Correlation analysis was performed using Pearson's
464 correlation.

465

466

467

468

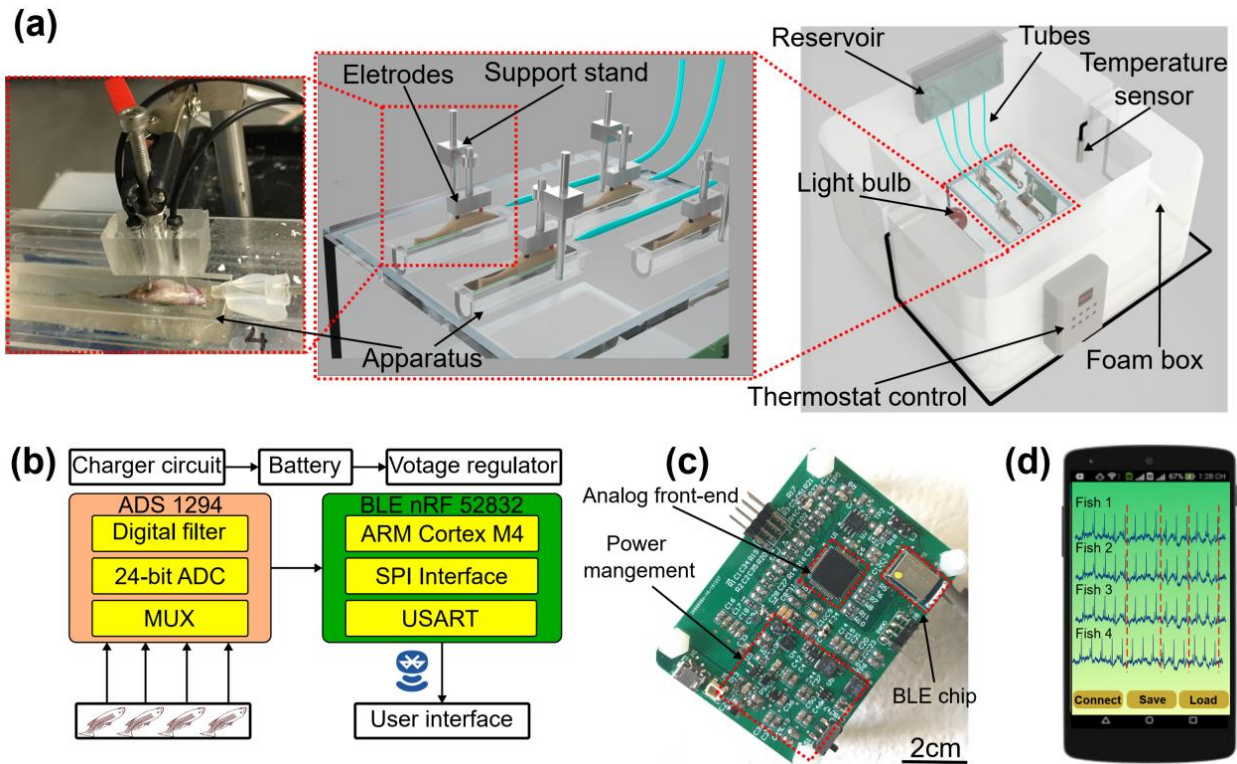
469

470

471

472

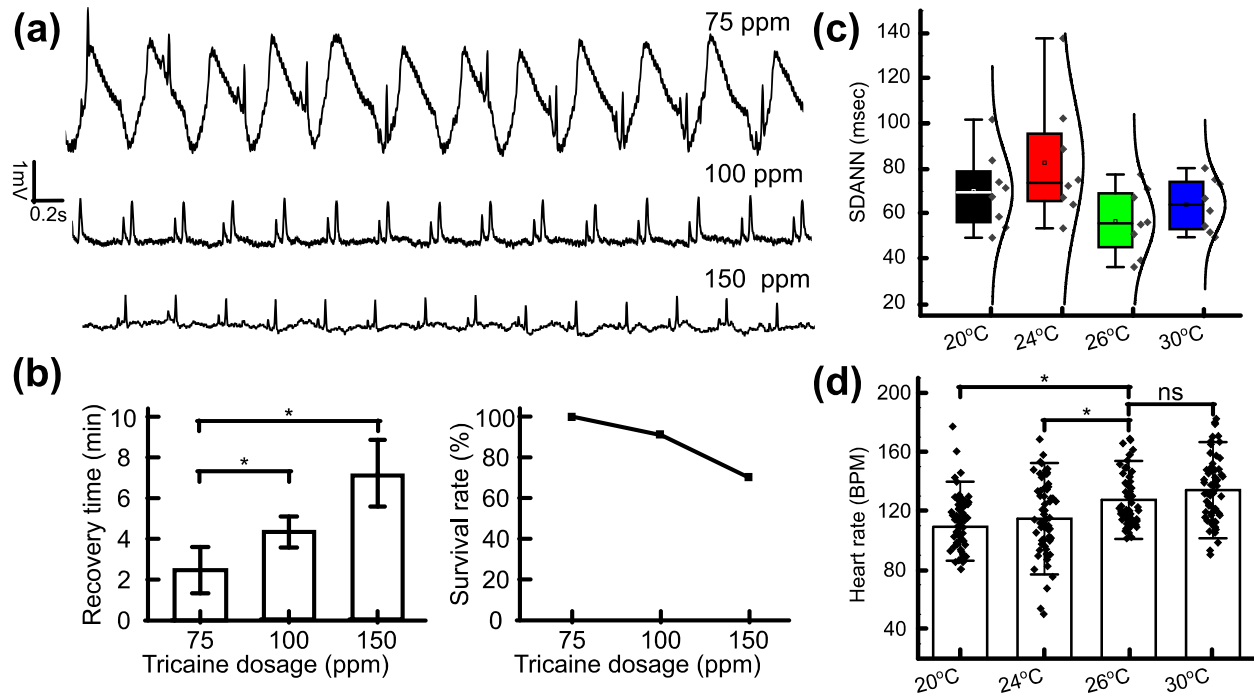
473



474

475 **Figure 1.** Design of the prolonged ECG system for multiple adult zebrafish recording. (a) the
476 prolonged ECG mechanical design: the reservoir containing solution, the tube system dropping
477 the solution on the fish, the electrode and support stand recording the ECG signal. (b) System-
478 level block diagram showing analog front-end chip, signal transduction, wireless transmission for
479 the ECG signal to user interface. (c) In-house electronic board having system-on-chip for wireless
480 transmission, power management connecting to the electrode for ECG acquisition. (d) User
481 interface of mobile application receiving ECG signal from multiple fish.

482



483

484 **Figure 2.** Investigation of tricaine and temperature to reduce cardiac rhythm side effect. (a) ECG
485 morphology example recorded by different Tricaine concentrations. (b) Bar chart comparing
486 recovery time needed after treatment for each Tricaine concentration. Line graph describing the
487 survival rate of zebrafish treated by different Tricaine concentrations. (c) SDANN in WT fish with
488 different temperatures. (d) Heart rate in WT fish with different temperatures. *p < 0.05; **p < 0.01
489 (one-way analysis of variance). ns indicates not significant.

490

491

492

493

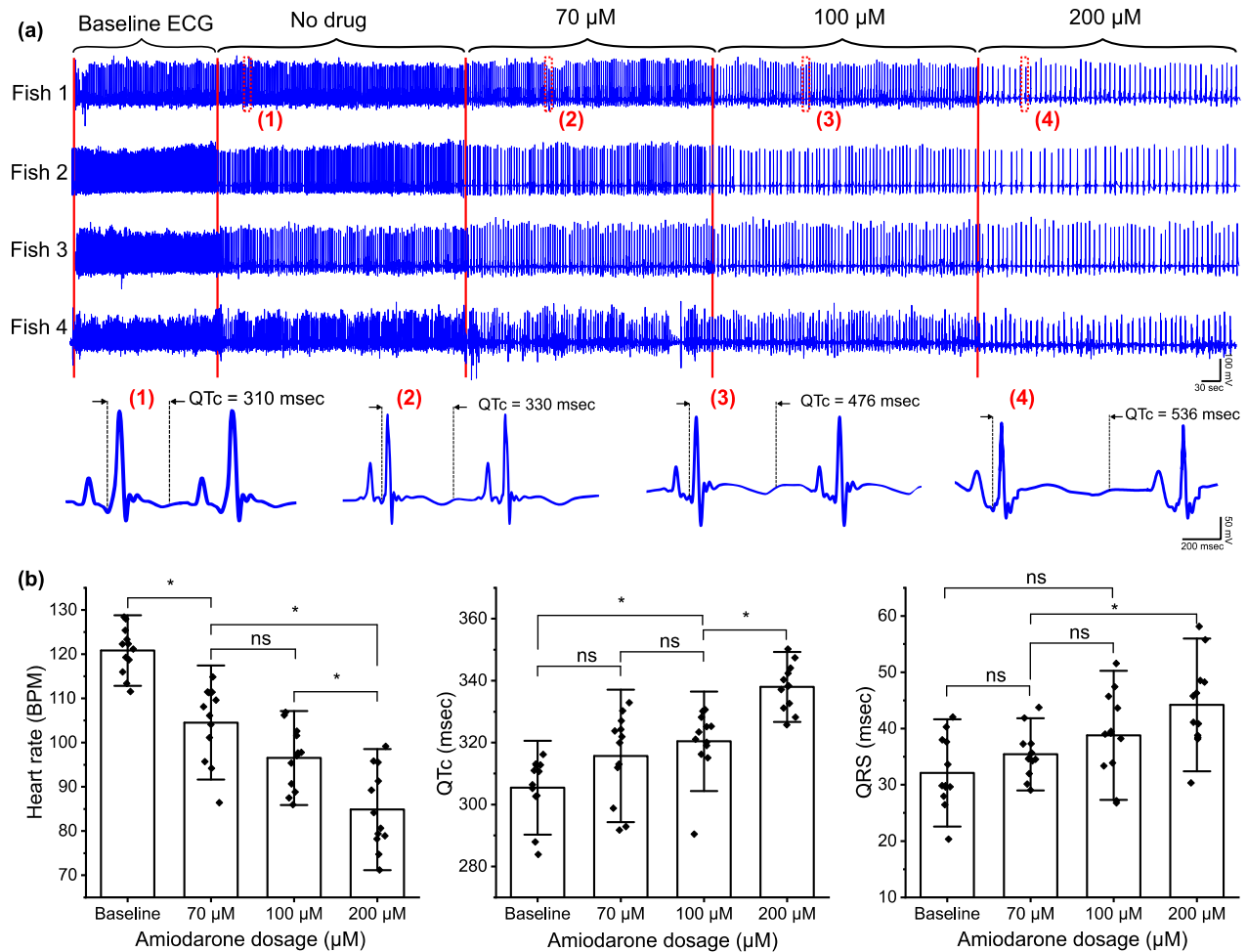
494

495

496

497

498



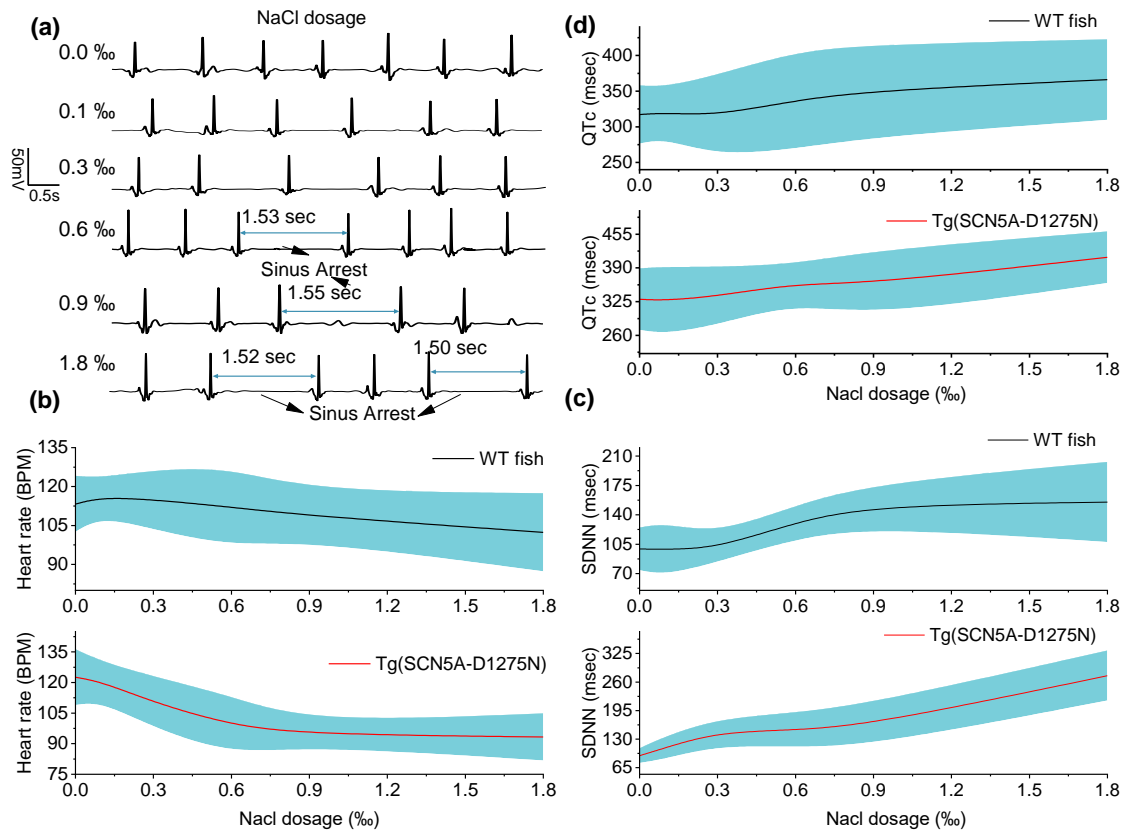
499

500 **Figure 3.** Demonstration of the prolonged ECG system showing the ECG morphology in response
501 to different amiodarone concentrations. (a) The representative of ECG signal recorded by the
502 proposed system and its change of signal morphology due to different amiodarone dosages in
503 real time. (b) Bar chart describing the discrepancy of HR value, QTc interval and QRS interval in
504 ECG signal with different amiodarone dosages (n = 8 fish). *p < 0.05 (one-way analysis of variance
505 with Turkey test). ns indicates not significant.

506

507

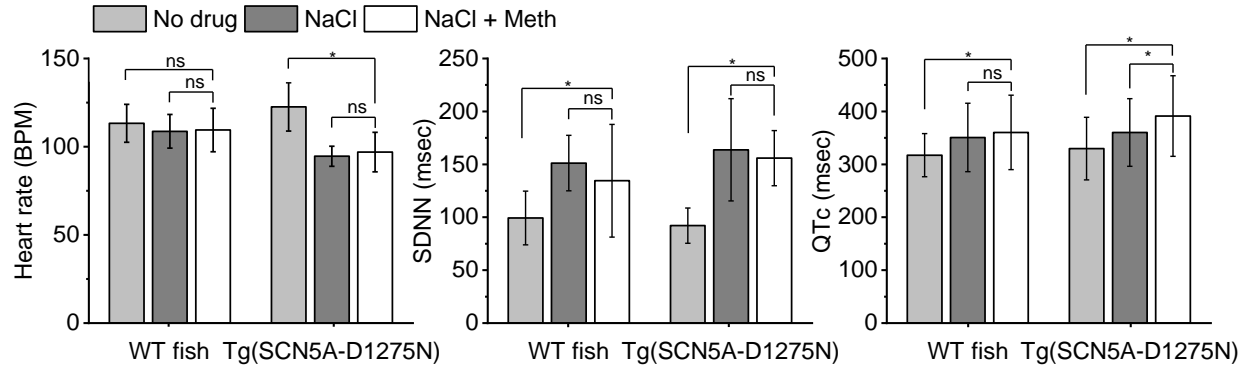
508



509

510 **Figure 4.** Evaluation of Na⁺ sensitivity in the development of sinus arrest in *Tg(SCN5A-D1275N)*
511). (a) the representative ECG waveforms before and after NaCl treatment with different dosages.
512 The sinus arrest is to be appear more in response to the increase of the NaCl dosage. (b) the
513 average heart rate of wild-type fish (n = 12) and mutant fish (n = 8) with each dosage of NaCl. (c)
514 Standard deviation of normal-normal beat sinus (SDNN) of wild-type fish and mutant fish. (d) QTc
515 values of two types of fish after treatment with different NaCl concentration.

516



517

518 Figure 5. Investigation of methamphetamine (Meth)'s efficacy to rescue the heartbeat sinus after
519 treatment with NaCl. The experiment was analyzed and compared heart rate, QTc and SDNN
520 among three stages (i.e., no drug treatment, with NaCl and with NaCl + Meth) and the experiment
521 was conducted in both WT fish and mutant fish Tg(*SCN5A-D1275N*).

522

523

524

525

526

527

528

529

530

531

532

533

534

535

536

537

538

539

540

541

542

543

Table I

Fish	WT				Tg(<i>SCN5A-D1275N</i>)			
Drug	Average HR (BPM)	Percentage of Fish with SA (No. of cycles)	SA frequency epm	QTc (msec)	Average HR (BPM)	Percentage of Fish with SA (No. of cycles)	SA frequency epm	QTc (msec)
0 ‰ NaCl	113.3 ± 10.8	8.3(1)	0.08	317.2 ± 40.7	122.6 ± 13.7	12.5 (1)	0.125	329.8 ± 59.1
0.1‰ NaCl	115.9 ± 7.5	8.3(1)	0.08	319.7 ± 36.3	120.4 ± 9.9	12.5(1)	0.125	327.2 ± 64.8
0.3‰ NaCl	114.9 ± 11.5	8.3(1)	0.08	316.1 ± 56.6	110.3 ± 12.6	37.5(7)	0.875	335.7 ± 55.8
0.6‰ NaCl	112.1 ± 15.2	16.6(2)	0.16	337.2 ± 68.2	98.9 ± 14.4	75(8)	1	359.9 ± 37.1
0.9‰ NaCl	108.7 ± 9.5	25(3)	0.25	350.7 ± 64.7	94.6 ± 5.7	75(15)	1.875	360.1 ± 64.0
1.8‰ NaCl	102.4 ± 15.0	50(7)	0.42	366.1 ± 56.4	93.3 ± 11.5	87.5(17)	2.125	410.5 ± 49.5
0.9‰ NaCl + 50 µM Meth	109.4 ± 12.3	25(3)	0.25	360.2 ± 70.3	96.95 ± 21.2	75(15)	1.875	391.3 ± 76.1

544

545

546 [Acknowledgement](#)

547 The authors would like to acknowledge the financial support from the NSF CAREER Award
548 #1917105 (H.C.), the NSF #1936519 (J.L. and H.C), the NIH SBIR grant #R44OD024874
549 (M.P.H.L and H.C.), the NIH HL107304 and HL081753 (X.X.). We thank Lauren Schmiess-Heine
550 for managing the zebrafish facility; and staff members in the Xu lab at Mayo Clinic, MN, USA for
551 maintaining and sharing the *Tg(SCN5A-D1275N)* fish.

552

553 [Author Contributions](#)

554 Conceptualization: Tai Le, Anh Hung Nguyen, Hung Cao.

555 Data curation: Tai Le, Jimmy Zhang.

556 Formal analysis: Tai Le, Jimmy Zhang, Anh Hung Nguyen.

557 Investigation: Tai Le, Jimmy Zhang, Anh Hung Nguyen.

558 Methodology: Tai Le, Jimmy Zhang, Anh Hung Nguyen, Ramses Trigo, Khuong Vo.

559 Writing – original draft: Tai Le, Anh Hung Nguyen, Jimmy Zhang, Khuong Vo, Hung Cao.

560 Writing – review & editing: Tai Le, Jimmy Zhang, Anh Hung Nguyen, Khuong Vo, Michael P.H.
561 Lau, Juhyun Lee, Yonghe Ding, Xiaolei Xu, Hung Cao.

562 [References](#)

563

- 564 [1] S. S. Virani, A. Alonso, E. J. Benjamin, M. S. Bittencourt, C. W. Callaway, A. P. Carson,
565 *et al.*, "Heart Disease and Stroke Statistics—2020 Update: A Report From the American
566 Heart Association," *Circulation*, vol. 141, pp. e139-e596, 2020/03/03 2020.
- 567 [2] O. Monfredi and M. R. Boyett, "Sick sinus syndrome and atrial fibrillation in older persons
568 — A view from the sinoatrial nodal myocyte," *Journal of Molecular and Cellular Cardiology*,
569 vol. 83, pp. 88-100, 2015/06/01/ 2015.
- 570 [3] V. Adán and L. A. Crown, "Diagnosis and treatment of sick sinus syndrome," *Am Fam*
571 *Physician*, vol. 67, pp. 1725-32, Apr 15 2003.
- 572 [4] M. Semelka, J. Gera, and S. Usman, "Sick sinus syndrome: a review," *Am Fam Physician*,
573 vol. 87, pp. 691-6, May 15 2013.
- 574 [5] O. Aquilina, "A brief history of cardiac pacing," *Images in paediatric cardiology*, vol. 8, pp.
575 17-81, 2006.
- 576 [6] G. Gregoratos, M. D. Cheitlin, A. Conill, A. E. Epstein, C. Fellows, T. B. Ferguson, *et al.*,
577 "ACC/AHA Guidelines for Implantation of Cardiac Pacemakers and Antiarrhythmia
578 Devices: Executive Summary," *Circulation*, vol. 97, pp. 1325-1335, 1998/04/07 1998.
- 579 [7] M. R. Carrión-Camacho, I. Marín-León, J. M. Molina-Doñoro, and J. R. González-López,
580 "Safety of Permanent Pacemaker Implantation: A Prospective Study," *Journal of clinical*
581 *medicine*, vol. 8, p. 35, 2019.
- 582 [8] M. Y. Chung, S. M. Chae, and C. J. Kim, "Fatal cardiac thromboembolism in a patient with
583 a pacemaker during ureteroscopic lithotripsy for ureter stone: a case report," *Korean*
584 *journal of anesthesiology*, vol. 68, pp. 74-77, 2015.
- 585 [9] E. Sandgren, C. Rorsman, N. Edvardsson, and J. Engdahl, "Stroke incidence and
586 anticoagulation treatment in patients with pacemaker-detected silent atrial fibrillation,"
587 *PloS one*, vol. 13, pp. e0203661-e0203661, 2018.

- 588 [10] H. C. Patel and J. A. Mariani, "An overlooked case of pacemaker-related heart failure,"
589 *Echo Research and Practice*, vol. 4, pp. K57-K60, 01 Dec. 2017 2017.
- 590 [11] N. Kapoor, W. Liang, E. Marbán, and H. C. Cho, "Direct conversion of quiescent
591 cardiomyocytes to pacemaker cells by expression of Tbx18," *Nat Biotechnol*, vol. 31, pp.
592 54-62, Jan 2013.
- 593 [12] W. Ye, J. Wang, Y. Song, D. Yu, C. Sun, C. Liu, *et al.*, "A common Shox2-Nkx2-5
594 antagonistic mechanism primes the pacemaker cell fate in the pulmonary vein
595 myocardium and sinoatrial node," *Development (Cambridge, England)*, vol. 142, pp. 2521-
596 2532, 2015.
- 597 [13] W. M. H. Hoogaars, A. Engel, J. F. Brons, A. O. Verkerk, F. J. de Lange, L. Y. E. Wong,
598 *et al.*, "Tbx3 controls the sinoatrial node gene program and imposes pacemaker function
599 on the atria," *Genes & development*, vol. 21, pp. 1098-1112, 2007.
- 600 [14] M. L. Bakker, G. J. Boink, B. J. Boukens, A. O. Verkerk, M. van den Boogaard, A. D. den
601 Haan, *et al.*, "T-box transcription factor TBX3 reprogrammes mature cardiac myocytes into
602 pacemaker-like cells," *Cardiovasc Res*, vol. 94, pp. 439-49, Jun 1 2012.
- 603 [15] Y. F. Hu, J. F. Dawkins, H. C. Cho, E. Marbán, and E. Cingolani, "Biological pacemaker
604 created by minimally invasive somatic reprogramming in pigs with complete heart block,"
605 *Sci Transl Med*, vol. 6, p. 245ra94, Jul 16 2014.
- 606 [16] M. Choudhury, N. Black, A. Alghamdi, A. D'Souza, R. Wang, J. Yanni, *et al.*, "TBX18
607 overexpression enhances pacemaker function in a rat subsidiary atrial pacemaker model
608 of sick sinus syndrome," *J Physiol*, vol. 596, pp. 6141-6155, Dec 2018.
- 609 [17] L. Y, L. Y, Z. P, Z. J, and W. X, "New Strategies for the Treatment of Sick Sinus Syndrome,"
610 *Journal of Cardiology and Therapy 2020*, vol. 7(1), pp. 913-921, 2020.
- 611 [18] C. E. Genge, E. Lin, L. Lee, X. Sheng, K. Rayani, M. Gunawan, *et al.*, "The Zebrafish
612 Heart as a Model of Mammalian Cardiac Function," in *Reviews of Physiology,
613 Biochemistry and Pharmacology, Vol. 171*, B. Nilius, P. de Tombe, T. Gudermann, R.
614 Jahn, R. Lill, and O. H. Petersen, Eds., ed Cham: Springer International Publishing, 2016,
615 pp. 99-136.
- 616 [19] P. Nemtsas, E. Wettwer, T. Christ, G. Weidinger, and U. Ravens, "Adult zebrafish heart
617 as a model for human heart? An electrophysiological study," *Journal of Molecular and
618 Cellular Cardiology*, vol. 48, pp. 161-171, 2010/01/01/ 2010.
- 619 [20] K. Howe, M. D. Clark, C. F. Torroja, J. Torrance, C. Berthelot, M. Muffato, *et al.*, "The
620 zebrafish reference genome sequence and its relationship to the human genome," *Nature*,
621 vol. 496, pp. 498-503, 2013/04/01 2013.
- 622 [21] M.-H. Lin, H.-C. Chou, Y.-F. Chen, W. Liu, C.-C. Lee, L. Y.-M. Liu, *et al.*, "Development of
623 a rapid and economic in vivo electrocardiogram platform for cardiovascular drug assay
624 and electrophysiology research in adult zebrafish," *Scientific Reports*, vol. 8, p. 15986,
625 2018/10/30 2018.
- 626 [22] G. H. Chaudhari, K. S. Chennubhotla, K. Chatti, and P. Kulkarni, "Optimization of the adult
627 zebrafish ECG method for assessment of drug-induced QTc prolongation," *Journal of
628 Pharmacological and Toxicological Methods*, vol. 67, pp. 115-120, 2013/03/01/ 2013.
- 629 [23] C. C. Liu, L. Li, Y. W. Lam, C. W. Siu, and S. H. Cheng, "Improvement of surface ECG
630 recording in adult zebrafish reveals that the value of this model exceeds our expectation,"
631 *Scientific Reports*, vol. 6, p. 25073, 04/29/online 2016.
- 632 [24] M. R. Stoyek, E. A. Rog-Zielinska, and T. A. Quinn, "Age-associated changes in electrical
633 function of the zebrafish heart," *Progress in biophysics and molecular biology*, vol. 138,
634 pp. 91-104, 2018/10// 2018.
- 635 [25] F. Yu, Y. Zhao, J. Gu, K. L. Quigley, N. C. Chi, Y.-C. Tai, *et al.*, "Flexible microelectrode
636 arrays to interface epicardial electrical signals with intracardial calcium transients in
637 zebrafish hearts," *Biomedical Microdevices*, vol. 14, pp. 357-366, 2012.

- 638 [26] H. Cao, F. Yu, Y. Zhao, X. Zhang, J. Tai, J. Lee, *et al.*, "Wearable Multi-Channel
639 Microelectrode Membranes for Elucidating Electrophysiological Phenotypes of Injured
640 Myocardium," *Integrative biology : quantitative biosciences from nano to macro*, vol. 6, pp.
641 789-795, 2014.
- 642 [27] M. Lenning, J. Fortunato, T. Le, I. Clark, A. Sherpa, S. Yi, *et al.*, "Real-Time Monitoring
643 and Analysis of Zebrafish Electrocardiogram with Anomaly Detection," *Sensors*, vol. 18,
644 p. 61, 2018.
- 645 [28] S.-J. Cho, D. Byun, T.-S. Nam, S.-Y. Choi, B.-G. Lee, M.-K. Kim, *et al.*, "Zebrafish as an
646 animal model in epilepsy studies with multichannel EEG recordings," *Scientific Reports*,
647 vol. 7, p. 3099, 2017/06/08 2017.
- 648 [29] G. E. Kochiadakis, E. M. Kanoupakis, N. E. Igoumenidis, H. E. Mavrakis, P. K. Kafarakis,
649 and P. E. Vardas, "Efficacy and safety of oral amiodarone in controlling heart rate in
650 patients with persistent atrial fibrillation who have undergone digitalisation," *Hellenic J*
651 *Cardiol*, vol. 46, pp. 336-40, Sep-Oct 2005.
- 652 [30] L. A. Siddoway, "Amiodarone: guidelines for use and monitoring," *Am Fam Physician*, vol.
653 68, pp. 2189-96, Dec 1 2003.
- 654 [31] M. Matthews and Z. M. Varga, "Anesthesia and euthanasia in zebrafish," *Ilar j*, vol. 53, pp.
655 192-204, 2012.
- 656 [32] J. Yan, H. Li, H. Bu, K. Jiao, A. X. Zhang, T. Le, *et al.*, "Aging-associated sinus arrest and
657 sick sinus syndrome in adult zebrafish," *PLOS ONE*, vol. 15, p. e0232457, 2020.
- 658 [33] S. Nagasawa, H. Saitoh, S. Kasahara, F. Chiba, S. Torimitsu, H. Abe, *et al.*, "Relationship
659 between KCNQ1 (LQT1) and KCNH2 (LQT2) gene mutations and sudden death during
660 illegal drug use," *Scientific reports*, vol. 8, pp. 8443-8443, 2018.
- 661 [34] B. L. Henry, A. Minassian, and W. Perry, "Effect of methamphetamine dependence on
662 heart rate variability," *Addict Biol*, vol. 17, pp. 648-58, May 2012.
- 663 [35] A. Mente, M. O'Donnell, S. Rangarajan, G. Dagenais, S. Lear, M. McQueen, *et al.*,
664 "Associations of urinary sodium excretion with cardiovascular events in individuals with
665 and without hypertension: a pooled analysis of data from four studies," *The Lancet*, vol.
666 388, pp. 465-475, 2016.
- 667 [36] O. Campuzano, G. Sarquella-Brugada, A. Fernandez-Falgueras, M. Coll, A. Iglesias, C.
668 Ferrer-Costa, *et al.*, "Reanalysis and reclassification of rare genetic variants associated
669 with inherited arrhythmogenic syndromes," *EBioMedicine*, vol. 54, p. 102732, Apr 2020.
- 670 [37] I. G. Huttner, G. Trivedi, A. Jacoby, S. A. Mann, J. I. Vandenberg, and D. Fatkin, "A
671 transgenic zebrafish model of a human cardiac sodium channel mutation exhibits
672 bradycardia, conduction-system abnormalities and early death," *J Mol Cell Cardiol*, vol.
673 61, pp. 123-32, Aug 2013.
- 674 [38] J. Yan, H. Li, H. Bu, K. Jiao, A. X. Zhang, T. Le, *et al.*, "Aging-associated sinus arrest and
675 sick sinus syndrome in adult zebrafish," *PloS one*, vol. 15, pp. e0232457-e0232457, 2020.
- 676 [39] H. L. Tan, M. T. Bink-Boelkens, C. R. Bezzina, P. C. Viswanathan, G. C. Beaufort-Krol, P.
677 J. van Tintelen, *et al.*, "A sodium-channel mutation causes isolated cardiac conduction
678 disease," *Nature*, vol. 409, pp. 1043-7, Feb 22 2001.
- 679 [40] M. Liu, K.-C. Yang, and S. C. Dudley, "Cardiac sodium channel mutations: why so many
680 phenotypes?," *Nature Reviews Cardiology*, vol. 11, pp. 607-615, 2014/10/01 2014.
- 681 [41] D. Darbar, P. J. Kannankeril, B. S. Donahue, G. Kucera, T. Stubblefield, J. L. Haines, *et*
682 *al.*, "Cardiac Sodium Channel (<i>SCN5A</i>) Variants Associated with Atrial Fibrillation,"
683 *Circulation*, vol. 117, pp. 1927-1935, 2008.
- 684 [42] W. P. McNair, G. Sinagra, M. R. G. Taylor, A. Di Lenarda, D. A. Ferguson, E. E. Salcedo,
685 *et al.*, "SCN5A Mutations Associate With Arrhythmic Dilated Cardiomyopathy and
686 Commonly Localize to the Voltage-Sensing Mechanism," *Journal of the American College*
687 *of Cardiology*, vol. 57, pp. 2160-2168, 2011/05/24/ 2011.

- 688 [43] T. P. Nguyen, D. W. Wang, T. H. Rhodes, and A. L. George, "Divergent Biophysical
689 Defects Caused by Mutant Sodium Channels in Dilated Cardiomyopathy With
690 Arrhythmia," *Circulation Research*, vol. 102, pp. 364-371, 2008.
- 691 [44] C. Antzelevitch, "Brugada syndrome," *Pacing and clinical electrophysiology : PACE*, vol.
692 29, pp. 1130-1159, 2006.
- 693 [45] Y. Mizusawa and A. A. M. Wilde, "Brugada Syndrome," *Circulation: Arrhythmia and*
694 *Electrophysiology*, vol. 5, pp. 606-616, 2012.
- 695 [46] A. L. George, Jr., "Inherited disorders of voltage-gated sodium channels," *The Journal of*
696 *clinical investigation*, vol. 115, pp. 1990-1999, 2005.
- 697 [47] A. Gatouillat, Y. Badr, B. Massot, and E. Sejdić, "Internet of Medical Things: A Review of
698 Recent Contributions Dealing With Cyber-Physical Systems in Medicine," *IEEE Internet*
699 *of Things Journal*, vol. 5, pp. 3810-3822, 2018.
- 700 [48] Y. A. Qadri, A. Nauman, Y. B. Zikria, A. V. Vasilakos, and S. W. Kim, "The Future of
701 Healthcare Internet of Things: A Survey of Emerging Technologies," *IEEE*
702 *Communications Surveys & Tutorials*, vol. 22, pp. 1121-1167, 2020.
- 703 [49] T. Le, M. Lenning, I. Clark, I. Bhimani, J. Fortunato, P. Marsh, *et al.*, "Acquisition,
704 Processing and Analysis of Electrocardiogram in Awake Zebrafish," *IEEE Sensors*
705 *Journal*, vol. 19, pp. 4283-4289, 2019.
- 706 [50] Y. H. Chen, H. C. Lee, R. J. Hsu, T. Y. Chen, Y. K. Huang, H. C. Lo, *et al.*, "The toxic
707 effect of Amiodarone on valve formation in the developing heart of zebrafish embryos,"
708 *Reprod Toxicol*, vol. 33, pp. 233-44, Apr 2012.
- 709 [51] M. B. Rook, M. M. Evers, M. A. Vos, and M. F. A. Bierhuizen, "Biology of cardiac sodium
710 channel Nav1.5 expression," *Cardiovascular Research*, vol. 93, pp. 12-23, 2011.
- 711 [52] W. Li, L. Yin, C. Shen, K. Hu, J. Ge, and A. Sun, "SCN5A Variants: Association With
712 Cardiac Disorders," *Frontiers in Physiology*, vol. 9, 2018-October-09 2018.
- 713 [53] T. Le, J. Zhang, X. Xia, X. Xu, I. Clark, L. Schmiess-Heine, *et al.*, "Continuous
714 Electrocardiogram Monitoring in Zebrafish with Prolonged Mild Anesthesia," in *2020 42nd*
715 *Annual International Conference of the IEEE Engineering in Medicine & Biology Society*
716 *(EMBC)*, 2020, pp. 2610-2613.
- 717 [54] P. Sun, Y. Zhang, F. Yu, E. Parks, A. Lyman, Q. Wu, *et al.*, "Micro-Electrocardiograms to
718 Study Post-Ventricular Amputation of Zebrafish Heart," *Annals of Biomedical Engineering*,
719 vol. 37, pp. 890-901, 2009/05/01 2009.
- 720 [55] M. Maricondi-Massari, A. L. Kalinin, M. L. Glass, and F. T. Rantin, "The effects of
721 temperature on oxygen uptake, gill ventilation and ecg waveforms in the nile tilapia,
722 *Oreochromis niloticus*," *Journal of Thermal Biology*, vol. 23, pp. 283-290, 1998/10/01/
723 1998.
- 724 [56] C. A. MacRae and R. T. Peterson, "Zebrafish as tools for drug discovery," *Nature Reviews*
725 *Drug Discovery*, vol. 14, pp. 721-731, 2015/10/01 2015.
- 726 [57] J. Gehrig, G. Pandey, and J. H. Westhoff, "Zebrafish as a Model for Drug Screening in
727 Genetic Kidney Diseases," *Frontiers in Pediatrics*, vol. 6, 2018-June-28 2018.
- 728 [58] S. Cassar, I. Adatto, J. L. Freeman, J. T. Gamse, I. Iturria, C. Lawrence, *et al.*, "Use of
729 Zebrafish in Drug Discovery Toxicology," *Chemical research in toxicology*, vol. 33, pp. 95-
730 118, 2020.
- 731 [59] F. Shaffer and J. P. Ginsberg, "An Overview of Heart Rate Variability Metrics and Norms,"
732 *Frontiers in Public Health*, vol. 5, 2017-September-28 2017.